A Pilot-Vehicle Systems Approach to Longitudinal Flight Director Design

D. T. McRuer,* D. H. Weir,† and R. H. Klein‡
Systems Technology Inc., Hawthorne, Calif.

Recent developments in the theory of manual control displays lead to principles for analytical design of flight directors, given the dynamics of the (augmented) vehicle and its manual control system. The theory shows that there are effective director–vehicle controlled element dynamics which are preferred from the standpoint of pilot response and system performance. Other considerations include response compatibility, display consistency, and autopilot monitoring. This leads to rules and analytical procedures which allow the director computer feedbacks to be selected, weighted, and equalized to provide an effective director–vehicle system which satisfies both pilot-centered and guidance and control requirements. This paper summarizes the requirements and illustrates the analytical process for longitudinal control of transport-type aircraft during landing approach.

Introduction

THIS paper applies the existing "theory of manual control displays"[1–5] to obtain design principles for advanced flight director systems and illustrates their application with a landing-approach example. The feedback control system aspects of the director-pilot-vehicle system are considered as a whole. This impacts primarily on the director computer where the weighting and equalization of feedback signals occurs. Selecting the computer functions involves the following considerations: adequate guidance and control properties, controlled element dynamics (effective vehicle/director) which minimize the equalization and gain adjustment demands on the pilot, command signals which induce compatible vehicle responses when the pilot closes the loop, and displayed signals which are internally consistent and compatible with the external visual field. This analytical development emphasizes the longitudinal landing approach task from beam acquisition to flare initiation; but the evolved design principles can be extended to attitude hold, altitude hold, flare, and lateral path following tasks.

Following a background note, two kinds of requirements for director design are presented. Those related to basic guidance and control considerations, and those which result from the presence of a human pilot in the control loop. Two analytical examples illustrate the implementation of these requirements in the design of the director computer. The first example is a basic director (containing only pitch attitude and beam deviation) which satisfies some of the requirements. Its deficiencies motivate the synthesis of an advanced director (containing properly equalized additional feedbacks) which best satisfies both types of requirements.

Background

An approach flight director system combines display, computation, pilot, and effective (augmented) vehicle in a feedback control system, Fig. 1. The command elements in the director display provide lateral and vertical steering signals, made up of a combination of desired path and aircraft motion quantities. These are shaped, filtered and mixed appropriately to permit the pilot to close the flight director system loop with ease and efficiency. The status information includes an artificial horizon for all-purpose use, and other pictorial information pertinent to a particular phase of flight. In landing approach, localizer and glide path signals are presented and the more modern instruments also indicate altitude and airspeed error.

The nub of the dynamic design problem is the selection of the appropriate mix of signals to make up the steering commands. Historically, this has been done by displaying the output of an automatic control system, or by mechanizing the director computer based on guidance and control requirements and adjusting the feedbacks during simulation and flight test for acceptable pilot opinion and system performance. Both satisfy the guidance and control requirements, and the first is useful for monitoring; but neither pays explicit attention to the human pilot's needs until the system is tested or simulated. Time and money can be saved by considering the pilot's properties at the onset, and designing the director system for: minimum pilot-induced remnant (unwanted control action); minimum pilot effective time delay; wide range of pilot gain to permit either very loose or very tight control with resulting good closed-loop characteristics; and best pilot opinion. The fundamental requirements (for human or automatic controller) and the human centered requirements, are developed in the next two sections. These are followed by an example of the analytical synthesis procedure.

Guidance and Control Requirements

The guidance and control requirements are to establish the aircraft on glide path, and to reduce any path errors to zero in a stable, well-damped and rapid manner. These requirements lead to outer loop feedbacks which are required to accomplish the mission, plus inner loop feedbacks which permit the first to function. The basic system for longitudinal control is shown in Fig. 2.

Beam deviation, d_e, is fundamental and it is corrupted by beam bends and noise in the airborne equipment. The actual signal is a glide path error angle, γ_e, converted from the deviation by the decreasing range, R. The path error and inner loop feedbacks are combined in the director com-

Presented as Paper 70-1001 at the AIAA Guidance, Control and Flight Mechanics Conference, Santa Barbara, Calif., August 17–19, 1970; submitted September 18, 1970; revision received April 16, 1971. This paper includes research efforts supported by the Ames Research Center, NASA, Moffett Field, Calif., under Contract NAS2-3746.

Index categories: Aircraft Subsystem Design; Aircraft Landing Dynamics; Navigation, Control, and Guidance Theory.

* President and Technical Director. Fellow AIAA.
† Principal Research Engineer. Member AIAA.
‡ Senior Research Engineer. Member AIAA.

puter and displayed to the pilot. The pilot may close other loops using raw data from the instrument panel, but these are unnecessary if the director is properly designed. To avoid pilot gain reduction with decreasing range, the time-varying gain G_{γ_e} is multiplied by the range to obtain a constant coefficient G_{d_e}.

Table 1 summarizes the feedbacks in the computed director signal which can satisfy the system functions. These are generally known and they are elaborated in the analysis example. Beam deviation is the basic outer loop, and its gain determines the bandwidth of the system. Attitude, rate of climb, and/or beam rate provide damping. Pitch attitude functions to maintain attitude stability and avoiding over-rotation. Regulation against winds (windproofing) is accomplished by adding various functions of beam deviation. Integral of beam deviation reduces path errors in the presence of very low-frequency beam commands or wind shears.

Pilot Related Requirements

The presence of a human pilot in the control loop requires a division of functions between the pilot and the director computer. The feedbacks must be selected, equalized, and weighted, not only for good performance, but to be compatible with good pilot ratings.

Equalization for Minimum Pilot Effort

The human pilot adapts his characteristics to compensate for dynamic deficiencies of the effective controlled element. As part of this adaptation, he may develop low-frequency lead or adjust his gain precisely. The cost of low-frequency lead is increased pilot time delay, increased pilot remnant, and a degradation in pilot ratings.[8–10] These reduce system performance and spare cockpit workload capacity.

These human pilot properties imply that the effective controlled element should require no low-frequency lead equalization and permit pilot loop closure using a range of pilot gains. This can be achieved when the effective controlled element approximates either a gain, K, or an integration, K/s, in the frequency range of pilot-director-vehicle system crossover. Although the pilot's effective time delay is somewhat less with a simple gain than with an integrator it is not feasible or desirable from other considerations to obtain the former in an approach director.

A K/s-like effective controlled element is nearly as good as a pure gain from the standpoint of pilot response and performance. With K/s the pilot-transfer characteristics are approximately a gain plus time delay in the frequency region of control, his time delay will be close to minimum, and remnant can be minimized with the proper choice of controlled element gain. Lead generation requirements are small, although the pilot can use a small amount at high-frequency to reduce his effective time delay in the loop. This lead can be minimized by making the controlled element more like a gain at high frequency.

Other requirements, based on minimizing pilot effort, are to range compensate the beam error to make the display controlled element dynamics approximately time invariant. The pilot can adjust to nonstationary situations, but it involves adaptation and learning which increases task difficulty and degrades performance, and to account for other pilot workload and for inattentive operation by providing dynamics which permit wide variations in pilot gain while retaining adequate gain and phase margins throughout the mid-frequency region. Thus conditionally stable systems and beam integral feedbacks are undesirable. These minimum pilot effort requirements must be further tempered with the considerations developed below.

Table 1 Summary of feedbacks to satisfy fundamental requirements

Systems functions—fundamental requirements	Flight director feedbacks
Path command and stiffening	Beam deviation, d
Path angle trimming	Beam integration, $\int d dt$
Curved path following	Beam double integration $\int(\int d dt)dt$
Path damping	Attitude θ at path frequencies; or beam rate $\dot{d}$; or rate of climb $\dot{h}$
Short-period attitude regulation	Attitude θ at short-period frequencies
Short-period damping	Attitude rate $\dot{\theta}$
Low-frequency windproofing	Beam integration, $\int d dt$
Mid-frequency windproofing	Beam rate $\dot{d}$ or rate of climb $\dot{h}$
High-frequency windproofing	Vertical acceleration, a_z

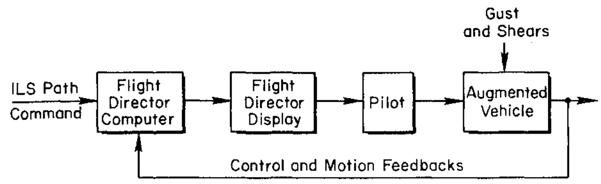

Fig. 1 Basic flight director system elements in approach.

Response Compatibility

Response compatibility considers the ways in which the various motions of the aircraft interrelate and how this affects the pilot. In essence, the airframe responses generated by the pilot in attempting to reduce the director error signal to zero should be similar to those which he experiences under other manual control conditions. This is desirable both for the pilot's internal self-monitoring functions and for the monitoring of pilot activity by the copilot using the full instrument panel. Quantitatively, this requirement can be assessed using modal response ratios as shown in the subsequent example. It also relates to the compatibility between the director display and the autopilot action during an automatic approach.

Face Validity and Command Bar Consistency

Some elements of the director display are intended as instrument reproductions of those portions of the external world which are sources of visual flight cues. If the resulting abstraction evokes responses while on IFR that are similar to those under VFR conditions the display is adequate from a behavioral standpoint, and it may even be superior to VFR by providing cues which are unavailable from the visual scene. In a director these cues are command signals which the pilot is to follow, and the rest of the display presents status information. If the status information corresponds to the actual situation, it has a high degree of face validity. For example, the artificial horizon corresponds directly with the actual horizon.

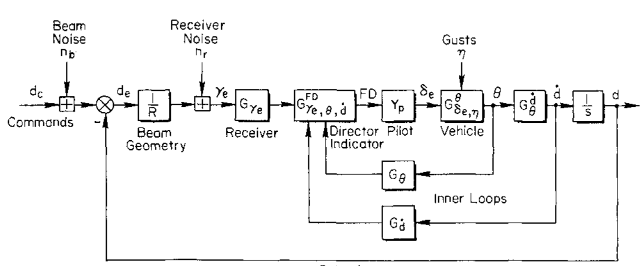

Fig. 2 Block diagram for approach control with flight director.

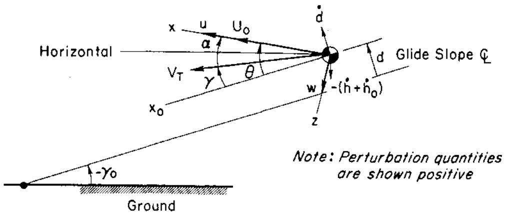

Fig. 3 Body axis system.

The command signals must also have face validity in some sense. In this case the cue is different from status information, because the command signal is a mixture of control and vehicle motions rather than an abstraction of one real world cue. However, some correspondence does exist between the command signal and the dominant vehicle motion or control quantity in each of several frequency bands. Thus, the command signal has some degree of consistency with the status elements on the display. This is necessary if the pilot is to believe his instruments. For example, the flight director should be dominated by attitude at short period frequencies but retain only beam deviation at low frequencies.

The integral of beam deviation is not a suitable component of the flight director command signal because it can result in a displayed low-frequency error when the aircraft is actually stabilized on the beam. In this sense the command would be inconsistent with the status information of the ILS indicator. This implies that the beam integration needed to satisfy such functions as low-frequency windproofing, curved path following, etc., must be accomplished by the pilot.

The opposite result is obtained if pitch attitude feedback, without washout, is used as a means to supply path damping. Then the command bar can be zero when the beam deviation and pitch attitude components are equal and opposite. Again, it would be inconsistent for the glide slope and artificial horizon status information to indicate the aircraft was not on glide path, while at the same time, the command bar was zero.

Director-computer requirements which consider pilot effort, response compatibility, and command bar consistency are summarized in Table 2. Together, the guidance and control and pilot-centered requirements prescribe the director computer feedbacks, and their weighting and equalization. The implementation and analytical interpretation of these requirements needed to accomplish a landing approach for a conventional transport-type aircraft is presented below.

Synthesis of an Advanced Longitudinal Director

The derivation of the director/vehicle controlled element is accomplished by setting up a system which has feedbacks that satisfy the functional requirements in a minimal way, and then subjecting it to constructive criticism. A minimum system is chosen on the basis of the steady-state path error in the presence of the following inputs: step offset from the beam; step changes in wind velocity; ramp changes in wind velocity along the beam. A system which accomplishes these functions is beam deviation plus washed-out pitch attitude. The deficiencies of this basic deviation attitude system provide the start for evolving an advanced director that has superior regulation and command following properties, and which better satisfies the pilot's subjective feelings. This is done by an analytical development using the DC-8 transport as a numerical example.

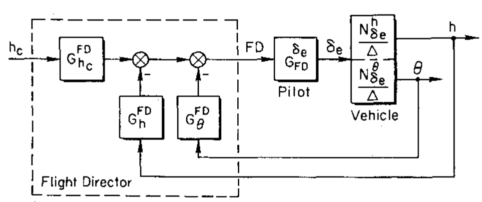

Fig. 4 Simplified director-vehicle block diagram.

Table 2 Flight director computer functions for human-centered requirements

Requirement	Function
K/s effective controlled	$\dot{h}$ or $\dot{d}$ feedback at mid-frequencies
Command Bar Consistency	Only d feedback at very low frequency. θ feedback at short period frequencies.
Response Compatibility	Response with flight director similar to that for raw data (or VFR); and similar to that for autopilot, i.e., θ and $\dot{h}$ inner loop feedbacks.

Axis System and Vehicle Equations

The analysis uses a conventional body-fixed stability axis system. For landing approach the unperturbed x-axis is aligned with the glide slope, making $\theta_o = \gamma_0$. When the aircraft's attitude is perturbed, the orientation of the body-fixed x and z-axes becomes that shown in Fig. 3.

The longitudinal dynamics of the vehicle are assumed to be described by the linearized three-degree-of-freedom perturbation equations given in Eq. (1).

$$\begin{bmatrix} s - X_u & -X_w & g\cos\Theta_0 \\ -Z_u & s - Z_w & -U_0 s + g\sin\Theta_0 \\ -M_u & -(M_{\dot{w}}s + M_w) & s(s - M_q) \end{bmatrix} \begin{bmatrix} u \\ w \\ \theta \end{bmatrix} = \begin{bmatrix} X_{\delta_e} \\ Z_{\delta_e} \\ M_{\delta_e} \end{bmatrix} [\delta_e] \quad (1)$$

$$\dot{d} = -w + U_0\theta + l_x\dot{\theta}, \text{ at station } l_x$$

$$\dot{h} = -w\cos\Theta_0 + u\sin\Theta_0 + U_0\cos\Theta_0\theta$$

$$a_z = \dot{w} - U_0\dot{\theta} + g\sin\Theta_0\theta - l_x\ddot{\theta}, \text{ at station } l_x$$

Values for the airframe parameters and stability derivatives for the DC-8 jet transport example are contained in Ref. 7. Numerical values for the transfer function numerators and denominators to be used in the example are given in Table 3.

Basic Beam-Deviation Plus Pitch Attitude System

The beam-deviation/attitude system is shown in the block diagram of Fig. 4, where G_h^{FD} and G_θ^{FD} are the respective feedback functions. The system has been made constant-coefficient by removing the range variation. Beam deviation d has been simplified to perturbation altitude, h, by assuming no steady-state wind effects to change the ground speed. Without wind, the small difference between d and h due to $\cos\Theta_0$ is negligible for glide path angles of current ILS systems.

A central implication of the pilot-centered requirements is that the gains and equalizations be selected so that the net transfer characteristics from elevator δ_e to director instrument displacement FD look approximately like an integration K/s. The analytical procedure for assessing and establishing this result is to add the component vehicle transfer functions with their associated equalization. The effective flight director transfer function is then,

$$FD/\delta_e = G_\theta^{FD}N_{\delta_e}^{\theta} + G_h^{FD}N_{\delta_e}^{h}/\Delta \quad (2)$$

For the basic system the feedback functions are:

$$G_\theta^{FD} = K_\theta s/s + 1/T_{WO}$$
$$G_{h_c}^{FD} = G_h^{FD} = K_h \quad (3)$$

The controlled element transfer function is then given by

$$\frac{FD}{\delta_e} = \frac{\dfrac{K_\theta A_\theta s}{s + 1/T_{WO}}\left(s + \dfrac{1}{T_{\theta_1}}\right)\left(s + \dfrac{1}{T_{\theta_2}}\right) + K_h \dfrac{A_{\dot{h}}}{s}\left(s + \dfrac{1}{T_{h_1}}\right)\left(s + \dfrac{1}{T_{h_2}}\right)\left(s + \dfrac{1}{T_{h_3}}\right)}{\Delta} \qquad (4)$$

The washout time constant is chosen to retain a good attitude signal at and below mid-frequency to ensure good path damping, but yet not too slow to allow a pitch angle change due to a steady wind to cause a standoff with the beam deviation. In order to obtain a closed-loop system that will have the required path damping as well as a closed-loop path mode frequency greater than the phugoid, the washout inverse time constant must be less than the phugoid, ω_p. With approach speeds on the order of 200 to 300 fps, the washout time constant will generally be around 10 sec, if not more.

With a very slow washout the numerator of Eq. 4 combines into a low-frequency dipole pair, $(s + 1/T_{WO})'/(s + 1/T_{WO})$, which cancel to a first approximation, a first-order root at nearly $1/T_{h_1}$, and a second-order pair at an undamped natural frequency, ω_θ, proportional to the $(K_h/K_\theta)^{1/2}$ gain ratio. The approximate transfer function is

$$\frac{FD}{\delta_e} \doteq \frac{K_\theta A_\theta (s + 1/T_{h_1}')[s^2 + (1/T_{\theta_2})s + K_h A_{\dot{h}}/K_\theta A_\theta T_{h_2} T_{h_3}]}{s[s^2 + 2\zeta_p \omega_p s + \omega_p^2][s^2 + 2\zeta_{sp}\omega_{sp} s + \omega_{sp}^2]} \qquad (5)$$

Figure 5 contains frequency response ($j\omega$-Bode) and root locus plots of this basic system transfer function for two values of the gain ratio, K_h/K_θ. The smaller value is given by the dashed line. Note that at larger K_h/K_θ values (solid line) the system is conditionally stable and has no region of K/s-like amplitude ratio. This will make the system very sensitive to variations in pilot gain, and will restrict the pilot-vehicle system crossover to frequencies outside the crosshatched unstable region. The system becomes unconditionally stable as ω_θ is decreased. Also, if ω_θ is decreased the spread between ω_θ and ω_{sp} increases and a small region of K/s-like amplitude ratio may be produced in between. As such, the form of the response is insensitive to changing gain and the bandwidth is proportional to the gain selected, whereas with K/s^2-like systems the closed-loop dynamics change markedly as the gain varies. The predominant K/s^2 nature of this effective controlled element in the anticipated crossover frequency region between the phugoid, ω_p, and short period, ω_{sp}, is the most apparent drawback of the beam deviation/pitch attitude flight director system.

Figure 5 and Eq. 5 show that with large enough pitch gain, K_θ, the second-order ω_θ zeros can be overdamped to produce two first-order zeros. This appears to improve the mid-frequency gain and produce the desirable K/s region, but it has limitations. The total numerator damping is constant so the two first orders cannot be placed separately in the most desirable locations. Also, for large attitude feedback gain the flight director will look very much like an amplified pitch attitude display, and be too busy in turbulence, violating the command bar consistency requirement. Attempts by the pilot to follow the bar may result in unacceptable normal accelerations and pitch attitude excursions—incompatible with accepted responses.

Other over-all deficiencies of the basic $\theta + h$ flight director include poor beam following in the presence of gusts due to the slow attitude washout, high sensitivity of the numerator zeros to slight changes in the K_h/K_θ ratio, and the K/s^2-like amplitude ratio above the short period. This implies a need for pilot (or other) lead equalization in this frequency range in order to extend the K/s region. Usually this will not be a strong requirement unless ω_{sp} is smaller than about 1 rad/sec. For lower short period frequencies, additional equalization in the director should be considered.

The advantages and deficiences of the attitude-beam deviation system are summarized in Table 4.

Table 3 Longitudinal body fixed stability axis transfer functions for the DC-8 in the landing approach configuration[a]

Denominator	Δ	$= [0.0865;\ 0.166][0.627;\ 1.23]$
Pitch numerator	$N_{\delta_e}^{\theta}$	$= -0.915(0.101)(0.646)$
Altitude rate numerator	$N_{\delta_e}^{\dot{h}}$	$= 9.25(0.0352)(4.42)(-3.63)$
Vertical gust numerator	$N_{w_g}^{\dot{h}}$	$= -0.72(0.871)[0.011;\ 0.254]$
	$N_{w_g}^{\theta}$	$= 0.004(-0.0087)(0.0378)$
Coupling numerator	$N_{w_g \delta_e}^{\dot{h}\ \theta}$	$= 0.649(0.092)$

[a] To simplify the notation, $A[s^2 + 2\zeta\omega s + \omega^2]$ is written $A[\zeta;\ \omega]$ and $A(s + a)$ is written $A(a)$.

Addition of Beam Rate Feedback to the Basic Director

Combining beam rate or washed out altitude rate with attitude and beam deviation feedbacks provides more precise beam following, and better fulfillment of pilot-centered requirements. The basic effect is to change the second-order zeros in the flight director transfer function of Eq. 5 to

$$[s^2 + (1/T_{\theta_2} + (K_{\dot{h}}/K_\theta)(A_{\dot{h}}/A_\theta)s + (K_h/K_\theta)(A_{\dot{h}}/A_\theta)] \qquad (6)$$

This quadratic§ may be separated into two independent first-order zeros. Each can be located independently to maximize the region of K/s-like amplitude ratio. This means placing them near ω_p and ω_{sp}, respectively. When the two roots are greatly different, Eq. 6 separates into one very small root, $-1/T_1$, given by

$$1/T_1 = (K_h Z_\alpha/K_\theta)/(1/T_{\theta_2} + K_{\dot{h}} Z_\alpha/K_\theta) \doteq (K_h Z_\alpha/K_\theta)/K_{\dot{h}} Z_\alpha/K_\theta[1 - K_\theta/U_0 K_{\dot{h}}] = K_h/K_{\dot{h}} \qquad (7)$$

and one large root $-1/T_2$ where

$$1/T_2 = -K_{\dot{h}} Z_\alpha/K_\theta[1 - K_\theta/U_0 K_{\dot{h}}] \doteq -K_{\dot{h}} Z_\alpha/K_\theta \qquad (8)$$

Figure 6 presents frequency response and root locus plots for the modified director–vehicle controlled element. The zeros have been located as follows:

$$1/T_1 \doteq K_h/K_{\dot{h}} \doteq \omega_p \qquad (9)$$

$$1/T_2 \doteq -K_{\dot{h}} Z_\alpha/K_\theta \doteq \omega_{sp} \qquad (10)$$

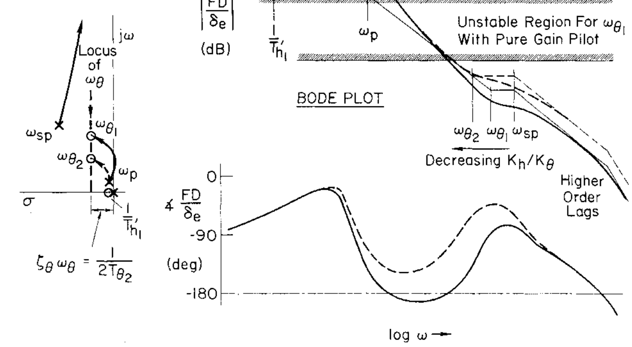

Fig. 5 Variation in director-vehicle properties with K_h/K_θ weighting.

§ The $1/T_{h_2}$ and $1/T_{h_3}$ zeros are assumed large relative to ω_{sp} and $A_{\dot{h}}^* = A_{\dot{h}}/T_{h_2}T_{h_3}$.

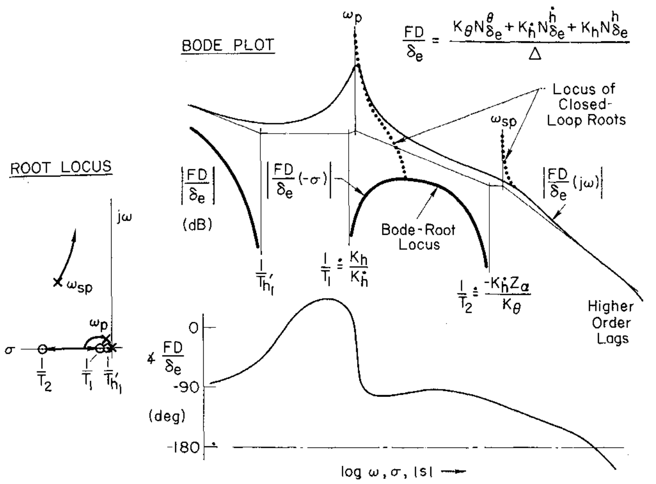

Fig. 6 Director-vehicle properties with beam rate added.

The frequency response shows a broad K/s region between ω_p and ω_{sp}, with very little phase dip near ω_p. The path damping is now coming from the low-frequency zero, $1/T_1$, due to the $\dot d$ (or $\dot h$) feedback. Good high-frequency properties are provided by the other zero, $1/T_2$.

The gust regulation and low-frequency windproofing are also improved with the addition of $\dot d$ or $\dot h$ because the attitude feedback can be washed out much faster than in the basic flight director case without compromising the mid-frequency path damping. The relationship between θ and $\dot h$ is helpful in determining the slowest reasonable pitch attitude washout time constant. In the low to mid-frequency region, a good approximation relating $\dot h$ and θ for elevator inputs is given by

$$\dot h/\theta = U_0/(T_{\theta_2}s + 1) \text{ (ft/sec/rad)} \quad (11)$$

For frequencies below $1/T_{\theta_2}$, $\dot h$ and θ feedbacks are redundant (in the absence of winds), so θ can be washed out with a time constant of T_{θ_2} from the standpoint of path damping. Because the pitch attitude feedback provides the required attitude stability, the fastest washout time constant is near the short-period frequency.

The effect of the washout location on the windproofing of the $h,\theta,\dot h$ director has been derived analytically in Ref. 7 by evaluating the closed-loop beam deviation to w_g transfer function:

$$d_e/w_g]_{FD\to\delta_e} = \{N_{w_g}{}^d + [K_\theta s/(s + 1/T_{WO})]N^{d\,\theta}_{w_g\delta_e}\}/ \{\Delta + [K_\theta s/(s + 1/T_{WO})]N^\theta_{\delta_e} + K_{\dot h}(s + K_h/K_{\dot h})N_{\delta_e}{}^d\} \quad (12)$$

The closed-loop deviation error responses for two values of washout location are shown by the Bode amplitude ratios in Fig. 7. The dashed curve is for a slow washout and the solid (lower) curve is for a fast washout. The difference in error is related to the area between the curves on Fig. 7 when plotted in linear rather than logarithmic coordinates.

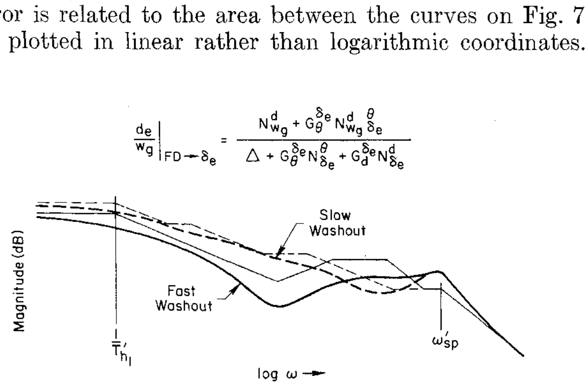

Fig. 7 Effect of pitch attitude washout on beam error due to *w*-gust.

Table 4 Relative properties of the basic deviation–attitude director system

Advantages	Deficiences
Simple to mechanize	K/s^2-like amplitude ratio at mid-frequency when K_h/K_θ weighting is acceptable
Provides command bar consistency with washed out attitude feedback	Poor windproofing due to slow washout
	K/s^2-like amplitude ratio at high frequency
	Maximum crossover frequency restricted by nonpilot lags in forward loop

As an example, if the w-gust is described by a low-frequency first-order power spectrum the mean square beam error for the fast washout case will be about a factor of two less than the same system with a slow washout.

The only deficiency with the combined $\theta,h,\dot h$ flight director system is that the K/s region of the open-loop FD/δ_e response does not extend beyond the short-period frequency. This means that potential high gain pilot closures will require pilot lead equalization in the vicinity of the short period.

Addition of Pitch Rate to the $\theta,h,\dot h$, Director

Pitch rate can be included in the G_θ^{FD} control path to independently control the short-period damping ratio. The addition of pitch rate creates an additional zero in the flight director transfer function, FD/δ_e. Placing the zero near the short period makes the flight director transfer function K/s-like at and above ω_{sp}. Also the closed-loop short-period damping ratio will then increase as the pilot increases his gain.

The resulting feedback functions including pitch rate are:

$$G_\theta{}^{FD} = K_\theta s/(s + 1/T_{WO}) + K_{\dot\theta}s = K_{\dot\theta}s[s + (1/T_{WO} + K_\theta/K_{\dot\theta})]/(s + 1/T_{WO}) \quad (13)$$

$$G_h{}^{FD} = K_h + K_{\dot h}s = K_{\dot h}(s + K_h/K_{\dot h}) \quad (14)$$

Combining these feedback functions results in a real zero, $1/T_1$ approximately equal to $K_h/K_{\dot h}$ and a complex pair, ω_θ, determined by the gain $K_{\dot h}/K_{\dot\theta}$. Numerical values are given in Table 5 for the DC-8 example. Selecting a $K_{\dot h}/K_{\dot\theta}$ value of $+0.011$ rad/ft places the complex pair of roots, ω_θ, near the vehicle short-period frequency to cancel ω_{sp} and extend the K/s region.

The open-loop director/vehicle, FD/δ_e, system survey is given in Fig. 8. The equalization terms ($1/T_1$ and ω_θ) do provide the desired K/s-like amplitude ratio over a large frequency region where the pilot should close the loop (the potential crossover region). The actual equalization terms (transfer function zeros) are compared with the approximate characteristic ratios in Table 6.

Pilot Loop Closure Considerations

In closing the loop, the pilot will introduce a time delay, and perhaps some offsetting high frequency lead. This will modify the open-loop system response properties as shown for an assumed pilot time delay, τ, of 0.4 sec by the dashed phase curve in Fig. 8. This gives the "maximum possible crossover" line which intersects the amplitude ratio plot at about 4 rad/sec. The potential crossover region is sketched in Fig. 8 indicating the frequency band (0.4 − 1 rad/sec) over which K/s-like controlled-element dynamics exist. Nominal pilot-vehicle system crossover will be near the middle of this band at about 0.6 rad/sec. The actual crossover will vary depending on the pilot, to satisfy the guidance and control requirements for particular inputs while at the same time maintaining an acceptable level of response compatibility (pitch attitude, load factor, etc.). His gain will

Table 5 Selected equalization values

Equalization	Expression	Desired location and vehicle value	Selected equalization	Remarks
Pitch washout	$\frac{1}{T_{WO}}$	$<\omega_{sp} = 1.23$ $>\frac{1}{T_{\theta_2}} = 0.65$	0.7	Washout less than ω_{sp} to provide attitude stability but greater than $1/T_{\theta_2}$ for windproofing and to maintain altitude bandwidth.
Pitch attitude	$\frac{1}{T_{WO}} + \frac{K_\theta}{K_{\dot\theta}}$	$\geq \omega_{sp} = 1.23$	1.7	Pitch attitude lead set to improve short period damping and extend the region of K/s by having the resulting ω_θ zeros cancel the ω_{sp} poles.
Altitude	$\frac{K_h}{K_{\dot h}}$	$\doteq \omega_p = 0.167$	0.2	Greater than ω_p to avoid a "busy" display and the low frequency closed-loop d/d_c amplitude droop, yet maintain mid-frequency phase margin.

Table 6 Comparison of approximate and exact equalization zeros

Equalization term	Characteristic ratio approximation	Calculated value
$1/T_1$	$K_h/K_{\dot h} = 0.20$	0.23
ω_θ	$[-Z_\alpha(K_{\dot h}/K_{\dot\theta})(1/T_{WO} + K_\theta/K_{\dot\theta})]^{1/2} = [(1.89)(1.7)]^{1/2} = 1.78$	1.27

also vary for different levels of system input (beam bends, turbulence) due to threshold effects. These are more detailed bases for the requirement to provide a broad range of K/s-like dynamics. Then the nature (mode shape) of the system response is insensitive to variations in pilot gain, whatever the cause, while the time characteristics change directly with gain.

For director control of transport aircraft in landing approach, a primary consideration in estimating pilot gain is the frequency and damping of the resulting closed-loop modes. The pilot will be sensitive to the pitch attitude response required in generating an altitude rate response needed to minimize beam error. One way to describe these characteristics quantitatively is with the use of modal response ratios. In general they have both an amplitude ratio and a phase. The closed loop response in a well-designed flight director system will be dominated by only a very few (3 or less) basic modes. These will be associated with the system crossover region.

Preferred values for the closed-loop modes can be illustrated with the loci of modal response ratios plotted in Fig. 9. The loci of modal response ratios plotted are $|\theta/\gamma|$, pitch attitude to path angle; equal to unity, and $|a_z/\theta|$, normal acceleration at the pilot relative to pitch attitude; equal to 0.1 g per degree. The plotted loci were obtained by evaluating the appropriate open-loop numerator ratios at possible closed-loop modes, and then plotting the frequency and damping associated with a given amplitude ratio (e.g., $|\theta/\gamma| = 1.0$). The loci form hypothetical boundaries for excessive pitch attitude and normal acceleration. Superimposing the example boundaries in Fig. 9 onto the root locus portion of Fig. 8 indicates the allowable gain region for the closed-loop modes. A crossover frequency of 0.6 rad-sec or less keeps the path mode accelerations due to attitude changes less than 0.1 g/deg, and the attitude to flight path angle change near unity at short-period frequencies. In other words, the roots on the complex locus in Fig. 8 lie within the example "acceptable" region in Fig. 9.

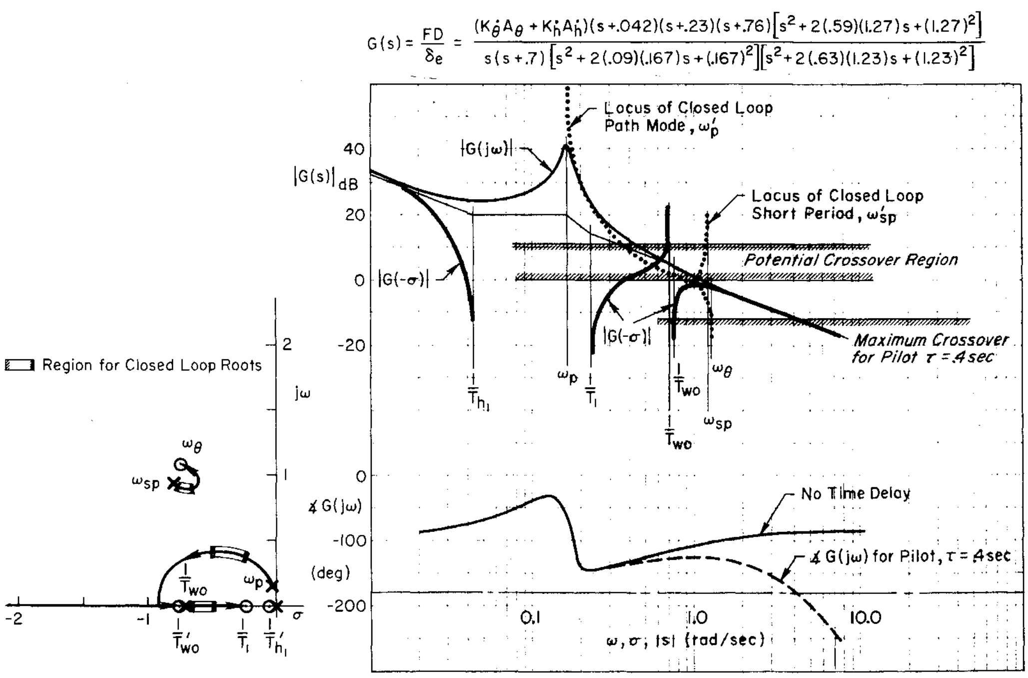

Fig. 8 Advanced pilot-director vehicle system.

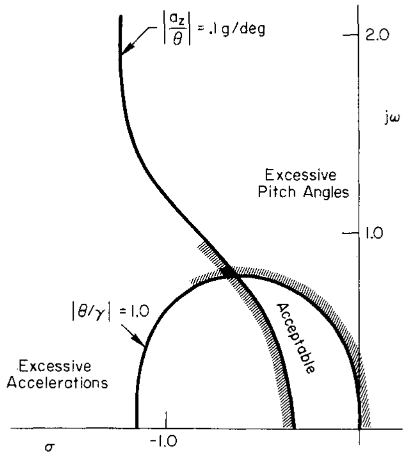

Fig. 9 Modal response ratio boundaries for the DC-8 example.

Another view of the closed-loop response compatibility for this example can be obtained from the beam deviation and pitch angle responses to beam commands. The frequency response plots for a 0.6 rad-sec crossover are shown in Fig. 10. The beam deviation response is flat out to the dominant mode and then rolls off sharply. The attitude response peaks up near the path mode and then rolls off sharply, indicating little attitude overshoot to an altitude command.

Other modal response ratios for this example are summarized in Table 7. The θ/h ratio can be used to express the attitude overshoot to an altitude command, by multiplying the θ/h ratio by the h/h_c response at the same mode. The small u/θ ratio at short period indicates that the vehicle holds speed well for short time intervals. Also at the path mode the speed changes will present little problem to the pilot.

In addition to the path and altitude modes, there will be a closed-loop root at low frequency as the free s at the origin is driven to $1/T_{h_1}'$ (see $|G(-\sigma)|$ on Fig. 8). Although this root is nearly canceled by the $1/T_{h_1}'$ zero in the closed-loop beam response there will be a significant response in airspeed. The airspeed settling time is nearly equal to $1/T_{h_1}$ and increases as the aircraft approaches the speed for minimum drag unless speed is separately controlled with the throttle.

In summary, modal response considerations show that the pilot gain and closed-loop properties can be estimated on the basis of what the pilot will consider to be a acceptable repertoire of system responses. This is somewhat different from the usual situation in which the analyst is attempting to estimate pilot gain and system stability margins largely on the basis of predicted path mode error. Unfortunately there are no hard data on acceptable values for the key modal response ratios for flight director or automatic landing systems. Presumably, the value of $|\theta/\gamma|_{s_i}$ for the dominant modes should be near unity to avoid overrotation in corrective maneuvers. As a practical matter, this is less of a problem with flight director systems than with automatic approach systems because the pilot is free to select the gain he feels is suitable in closing the loop.

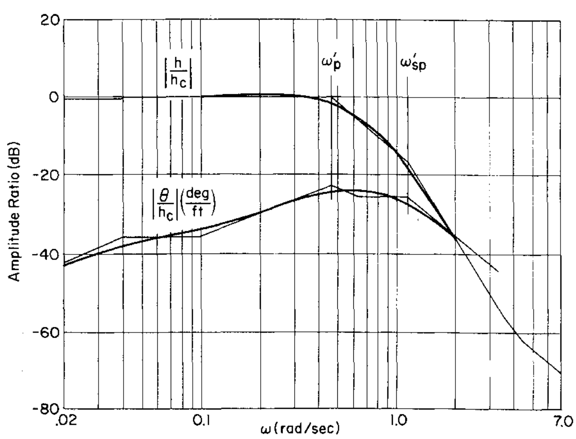

Fig. 10 Closed-loop attitude and altitude response to altitude commands for example crossover.

Table 7 Modal response ratios for example pilot closure

Modal response ratio	Closed-loop path mode [0.70; 0.44]	Closed-loop short period [0.62; 1.2]
θ/γ (deg/deg)	0.65 $\measuredangle$ 47°	1.15 $\measuredangle$ 90°
θ/h (deg/ft)	0.06 $\measuredangle$ 162°	0.32 $\measuredangle$ 225°
u/θ (ft/sec/deg)	1.75 $\measuredangle$ 19°	0.45 $\measuredangle$ −40°
a_z/θ (g/deg)	0.075 $\measuredangle$ 275°	0.09 $\measuredangle$ 200°

Conclusions

A set of principles, functional requirements, and analytical procedures can be defined for specifying and designing flight director-vehicle systems. These permit the designer to select, equalize, and weight the director feedbacks analytically, given the (augmented) vehicle dynamics and a definition of the task. This involves some tradeoff between the basic guidance and control requirements and additional requirements based on human pilot considerations. These new concepts include the following: 1—the effective director/vehicle controlled element should look like a K/s over a broad mid-frequency region, 2—the director display should be consistent with status information—low-frequency and steady-state bar motions should be beam deviation, the mid-frequency deviations should reflect corresponding vehicle motions, and high-frequency motions should be attenuated, 3—the compatibility of attitude and path motions has an important influence on pilot gain and system crossover frequency, and 4—scanning required to monitor status information will tend to reduce pilot gain and this can be avoided by suitably integrating the status information on the display.

By using these principles and analytical techniques the designer can 1—analytically set up the flight director during the design stage, 2—determine the interaction of system components (e.g., feedbacks, SAS, vehicle, display, pilot, etc.), 3—evaluate the trade off of guidance and control and pilot centered requirements, 4—predict pilot opinions and closed-loop performance, and 5—plan the final optimization process involving actual pilots in simulation and flight test more expeditiously. The result is a more efficient design process and a demonstrably superior director-pilot-vehicle system.

References

[1] McRuer, D., Jex, H. R., Clement, W. F., and Graham, D., "A Systems Analysis Theory for Displays in Manual Control," TR 163-1, AD 675 983, Oct. 1967 (revised June 1968), Systems Technology Inc., Hawthorne, Calif.

[2] Clement, W. F., Jex, J. R., and Graham, D., "A Manual Control-Display Theory Applied to Instrument Landings of a Jet Transport," *IEEE Transactions*, Vol. MMS-9, No. 4, Dec. 1968, pp. 93–110.

[3] Allen, R. W., Clement, W. F., and Jex, H. R., "Research on Display Scanning, Sampling, and Reconstruction Using Separate Main and Secondary Tracking Tasks," CR-1569, July 1970, NASA.

[4] Weir, D. H. and Klein, R. H., "The Measurement and Analysis of Pilot Scanning and Control Behavior During Simulated Instrument Approaches," CR-1535, June 1970, NASA.

[5] Clement, W. and Hofmann, L. G., "A Systems Analysis of Manual Control Techniques and Display Arrangements for Instrument Landing Approaches in Helicopters. Vol. I, Speed and Height Regulation," JANAIR Rept. 690718, AD 700 946, July 1969, Systems Technology Inc., Hawthorne, Calif.

[6] Johnson, W. A. and McRuer, D. T., "A System Model for Low-Level Approach," AIAA Paper 70-1034, Santa Barbara, Calif., 1970.

[7] Weir, D. H., Klein, R. H., and McRuer, D. T., "Principles for the Design of Advanced Flight Director Systems Based on the Theory of Manual Control Displays," CR-1748, March 1971, NASA.

[8] McRuer, D. T. and Jex, H. R., "A Review of Quasi-Linear Pilot Models," *IEEE Transactions*, Vol. HFE-8, No. 3, Sept. 1967, pp. 231–249.

[9] McRuer, D., Graham, D., Krendel, E., and Reisener, W., Jr., "Human Pilot Dynamics in Compensatory Systems—Theory, Models, and Experiments with Controlled Element and Forcing Function Variations," AFFDL-TR-65-15, July 1965, Air Force Flight Dynamics Lab., Wright-Patterson Air Force Base, Ohio.

[10] McRuer, D. and Weir, D. H., "Theory of Manual Vehicular Control," *Ergonomics*, Vol. 12, No. 4, 1969, pp. 599–663.

NOVEMBER 1971 J. AIRCRAFT VOL. 8, NO. 11

Measurement and Analysis of Pilot Scanning Behavior during Simulated Instrument Approaches

DAVID H. WEIR* AND RICHARD H. KLEIN†
Systems Technology, Inc., Hawthorne, Calif.

Experimental measurements of pilot scanning and control response in a simulated instrument approach are reported. Airline pilot subjects flew ILS approaches in a six degree-of-freedom fixed base DC-8 simulator at the NASA Ames Research Center. A conventional instrument panel and controls were used, with simulated vertical gust and glide slope beam bend forcing functions. Pilot eye fixations and scan traffic on the panel were measured using a recently developed eye point-of-regard (EPR) system. Simultaneous recordings were made of displayed signals, pilot response, and vehicle motions. The EPR data were reduced for 31 approaches with a cross section of subjects to obtain dwell times, look rates, scan rates, and fractional scanning workload. Flight director (zero reader) approaches as well as standard localizer/glide slope (manual) approaches were made. The scanning results showed the attitude and glide slope/localizer instruments to be primary in a manual ILS approach, sharing 70–80% of the pilot's attention. The glide slope/localizer instrument required shorter dwell times with a fixed instrument sensitivity. Differences in dwell time between pilots occurred mainly on the attitude instrument. With the flight director, glide path deviation errors were reduced and the flight director instrument dominated pilot attention (about 80%). There were no apparent circulatory scanning patterns in any of the approaches. These EPR results were generally consistent with prior data where meaningful comparisons could be made.

Introduction

FURTHER development and validation of the theory of manual control displays[1,2] required measurement and analysis of simultaneous eye movement and pilot response data in flight control tasks under realistic instrument conditions. The objective of the research program reported herein was to obtain such data for instrument approach tasks, and to reduce the eye point-of-regard (EPR) data to the scanning statistics needed to continue development of the theory. Data are now in hand for several airline pilots in more than a hundred simulated instrument approaches in a subsonic jet transport. The scanning statistics for a cross section of 31 two-minute runs are described and analyzed in this paper. They are part of the data base for ongoing efforts to correlate EPR with pilot response and displayed motion variables.

Presented as Paper 70-999 at the AIAA Guidance, Control and Flight Mechanics Conference, Santa Barbara, Calif., Aug. 17–19, 1970; submitted Sept. 11, 1970; revision received April 29, 1971. This paper includes research efforts supported by the NASA Ames Research Center, Moffett Field, Calif., under Contract NAS2-3746.

Index categories: Aircraft Handling, Stability, and Control; Research Facilities and Instrumentation.

* Principal Research Engineer. Member AIAA.

† Senior Research Engineer. Member AIAA.

Background

Early research in this area measured the instrument scanning patterns of pilots in a variety of actual IFR maneuvers,[4–8] but no records were made of the instrument readings or pilot responses. Stable statistical traffic patterns appeared in their results for various pilots and maneuvers. More recent research (Refs. 9–11) has been concerned mainly with statistical models of the scanning process, rather than with the establishment of connections with the causal factors of the displayed signals. Again, the displayed signals were either not recorded or not correlated against the scanning behavior, or the definition of the controlled element dynamics was incomplete.

These past studies have used eye movement cameras, electro-oculographics, or corneal reflection techniques; which tend to be expensive, difficult to operate, and detrimental to the experimental environment. An eye point-of-regard system recently developed by STI (Systems Technology Inc.) avoids many of these problems. It measures the horizontal and vertical movement of the eye with respect to the head by a corneal-schleral boundary contrast technique and the head movement relative to the panel reference by electromechanical means. These signals are combined in a special purpose computer to obtain overall eye point-of-regard. Figure 1 shows the device in use. This, plus proven